Phase Transitions in Dense Lipid Monolayers Grafted to a Surface: Monte Carlo Investigation of a Coarse-Grained Off-Lattice Model

F. M. Haas, R. Hilfer,† and Kurt Binder*

Institut für Physik, Johannes Gutenberg-Universität Mainz, D-55099 Mainz, Germany

Received: April 12, 1996; In Final Form: June 27, 1996[⊗]

Semiflexible amphiphilic molecules end-grafted at a flat surface are modeled by a bead-spring chain with stiff bond angle potentials. Constant density Monte Carlo simulations are performed varying temperature, density, and chain length of the molecules, whose effective monomers interact with Lennard-Jones potentials. For not too large densities and low temperatures the monolayer is in a quasi-two-dimensional crystalline state, characterized by uniform tilt of the (stretched) chains. Raising the temperature causes a second-order transition into a (still solid) phase with no tilt. For the first time, finite size scaling concepts are applied to a model of a surfactant monolayer, and it is found that the technique in this case again is useful to locate the transition more precisely. For comparison, also a one-dimensional version of the model is studied, and directions for future extensions of this modeling are discussed.

1. Introduction

Monolayers of surfactant molecules at surfaces have found widespread recent interest, since they have diverse potential applications for materials and possibly are model systems to understand more complex membranes.[1−7] Simple examples are provided by systems such as fatty acids ($CH_3(CH_2)_NCOOH$) at the air−water interface, the hydrophilic head groups being immersed into water while the hydrophobic alkane chains are stretched into the air (Figure 1). These rodlike non axially symmetric molecules give rise to a large variety of phases and phase transitions and have a very rich phase diagram.[6−11] The molecular origin of this complex phase behavior and the details of all these phase transitions are not yet fully understood (see, for example, ref 12). But a striking feature is that despite differences in detail, monolayers from fatty acids, phospholipids, alcohols, and esters exhibit a similar phase diagram.[7,8,10,11] This fact already suggests that full atomistic detail may not be necessary to understand the generic features of this phase behavior, and coarse-grained models may suffice to elucidate some of the mechanisms underlying the various phase transitions.

In this spirit we use for our computer simulations[13−16] a model (Figure 1) where we follow the idea of "coarse-graining" along the backbone of a polymer chain:[17−21] $n \approx 3-6$ successive CH_2 groups are integrated into one effective bond connecting effective monomers by (relatively) stiff springs. On this coarse-grained length scale, the fine structure of the torsional potential for the CH_2 units can be considered as washed out, and the stiffness of the semiflexible chain is described only in terms of a phenomenological potential for the angle between the effective bonds.[17−21] As is well-known (e.g. refs 20, 22), chain models without torsional potentials can be simulated about an order of magnitude more efficiently than those with torsion. An additional gain in efficiency results from the fact that the number of degrees of freedom is reduced in the coarse-graining: when the chemically realistic chain has a degree of polymerization of N, the coarse-grained chain has a degree of polymerization of only $l = N/n$.

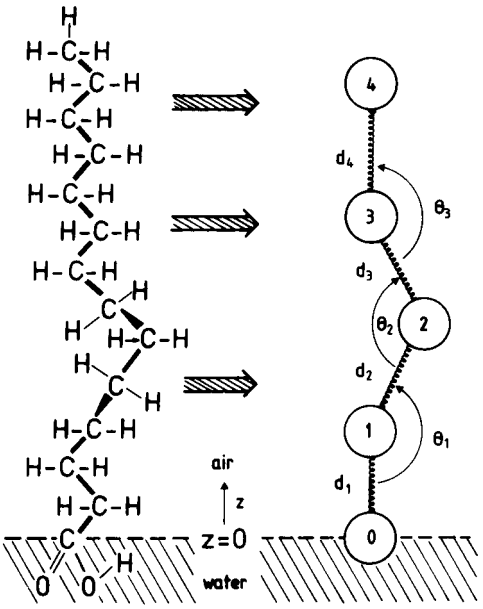

Figure 1. Schematic picture of a fatty acid at the air−water interface and the chosen coarse-grained model of the present paper, where we combine a number of $n \approx 3$ successive CH_2 groups into one effective monomer. The effective bonds between these effective monomers are represented by (stiff) springs. The persistence length of the alkane chain is controlled by an effective potential depending on the bond angle Θ_i, i being the label of the effective monomer, and d_i, the length of the effective bond between effective monomers i and $i-1$. Note that the hydrophilic group at the bottom labeled by $i = 0$ is represented by the same type of effective monomer as those chosen for the alkane chain, it differs from those only by the restriction that its perpendicular coordinate z is fixed at $z = 0$, the position of the air−water interface. Effective monomers also interact with Lennard-Jones potentials; see section 2.

Given the fact that for fatty acid monolayers the range of greatest interest is $12 \le N \le 22$, we work with $5 \le l \le 8$ (one effective monomer that is fixed at the surface plane represents the hydrophilic group, and hence only $l - 1 = 4-7$ effective monomers represent the alkane chain, cf. Figure 1.

Of course, there have been numerous previous simulation studies of both chemically realistic models[23−34] and idealized coarse-grained models[35−40] of such surfactant monolayers (and bilayers[34]). The atomistically detailed models clearly have an

† Present address: ICA, Universität Stuttgart, D-70569 Stuttgart, Germany.

[⊗] Abstract published in *Advance ACS Abstracts,* September 1, 1996.

S0022-3654(96)01098-2 CCC: $12.00

advantage in their chemically realistic description of dense packing of the atoms in the monolayer. However, molecular dynamics runs can be carried out for rather short time spans (less than a nanosecond) and small systems (typically on the order of 100 molecules) only; while in this way useful results on structural and dynamic properties in pure phases for parameters far off the phase transitions can be obtained, for the study of phase changes a much larger time range and larger sytems are mandatory.[41−43] Another difficulty is that the effective potentials to be used in chemically detailed descriptions of polymers and complex molecules are only inaccurately known.[18−20] On the other hand, coarse-grained models clearly lose some aspects of the physics that one wants to deal with: for example, treating the short alkane chains of the fatty acids as rigid rods (as done in refs 35, 36, and 38), one disregards melting of the layer and the associated intrachain conformational disorder. Treating the short alkane chain by a lattice model of semiflexible chains on cubic lattices, as done in refs 37, 39, and 40, one cannot describe the proper symmetry of any of the solid phases. While lattice models of polymers are rather good for long wavelength properties in dilute and semidilute solutions,[20] and hence can deal well with systems such as polymer brushes,[44−46] for the short alkane chains and high densities occurring in lipid monolayers we consider such lattice models as a crude caricature only, which suffer from various lattice artifacts.[40]

The model of Figure 1 hence should be viewed as a compromise in between these extreme choices. While our choice of fixing the head group exactly in one plane ($z = 0$) is a reasonable approximation for surfactants grafted at solid surfaces, as are also sometimes studied experimentally,[47−50] it suppresses vertical fluctuations, which clearly are important for surfactants at fluid interfaces; also our choice of the grafted end group having the same interactions as other effective monomers is a crude approximation, which deserves refinement in future work. A crucial shortcoming of our model, of course, is the cylindrical symmetry of our chains when they are stretched out in the *z*-axis: the corresponding all-trans zigzag-like configuration of the chemically realistic alkane chain lacks this symmetry. Hence in planes perpendicular to the *z*-axis herring-bone-like orientational ordering occurs, which cannot occur in our model where effective monomers lack a corresponding orientational degree of freedom.

Keeping in mind all these limitations of our model, it nevertheless can provide useful qualitative insight, as will become apparent in the following sections. We start (section 2) by defining the parameters of the model and briefly comment on the Monte Carlo simulation technique in the constant volume ensemble. Section 3 then discusses the continuous transition from the "uniform tilt" phase to the "no tilt" phase, paying attention to an analysis of finite size effects. Section 4 presents results describing the effects of varying the density of the monolayer, while section 5 reports the effects of varying the chain length. Section 6 contains our conclusions, while results on a corresponding one-dimensional version of our model are summarized in the Appendix.

2. The Model and the Simulation Technique

Here we specify the parameters of the coarse-grained model, shown already in Figure 1, that is used in our simulations.[13−15] Each surfactant molecule is represented by a bead-spring chain containing l effective monomers, with $l = 5-8$; typically $l = 7$ was chosen. As mentioned above, for a fatty acid molecule this should correspond to about 20 CH_2 groups in the alkane chain. The effective bond is represented by a finitely extensible but otherwise harmonic potential,

$$V_{\mathrm{bl}}(d_i) = c_{\mathrm{bl}}(d_i - d_0)^2, \quad \text{for} \quad |d_i - d_0| \le d_{\mathrm{bl}}, \quad i = 1, ..., l \tag{1}$$

$$V_{\mathrm{bl}}(d_i) = \infty, \quad \text{for} \quad |d_i - d_0| > d_{\mathrm{bl}} \tag{2}$$

Thus d_0 describes the distance between effective monomers for which the potential is minimal, d_{bl} is the maximal extension of the spring, and $2c_{\mathrm{bl}}$ its spring constant. The bond angle potential is chosen as

$$V_{\mathrm{ba}}(\Theta_i) = c_{\mathrm{ba}}[1 + \cos \Theta_i] \tag{3}$$

where $c_{\mathrm{ba}} > 1$ is the force constant (ensuring a minimum for $\Theta_i = \pi$, i.e. a fully stretched chain), Θ_i being the angle formed by the two bonds d_i, d_{i+1} (Figure 1).

All monomers except nearest neighbors along a chain interact with a Lennard-Jones potential. This potential is truncated at a distance $d_{\mathrm{LJ}}\sigma$ and shifted such that it vanishes at the truncation point. If ϵ is the interaction strength and σ its range, then

$$V_{\mathrm{LJ}}(r) = \begin{cases} \epsilon[(\sigma/r)^{12} - 2(\sigma/r)^6] - \epsilon(d_{\mathrm{LJ}}{}^{-12} - 2d_{\mathrm{LJ}}{}^{-6}), & r \le d_{\mathrm{LJ}}\sigma \\ 0, & r > d_{\mathrm{LJ}}\sigma \end{cases} \tag{4}$$

Note that the head groups ($i = 0$) interact with each other and with other effective monomers with the same potential, the only distinction being that the head groups are restricted to move in the surface plane, $z = 0$. This surface is ideally flat, structureless, and rigid, and hence at this level of idealization we do not distinguish whether the substrate is a fluid or a solid.

We choose dimensionless parameters by setting $\epsilon = 1$ and $\sigma = 1$. In these units the bond length d_0 is set to $d_0 = 0.7$. Remembering that in an alkane chain the C−C bond length is 1.53 Å and in an all-trans state of a chain stretched in the *z*-direction three successive C−C bonds correspond to a distance of about 3.5 Å, our length unit hence is about 5 Å. We then choose $d_{\mathrm{bl}} = 0.2$ (i.e. about 1 Å) and the cutoff for the nonbonded interaction $d_{\mathrm{LJ}} = 2$ (i.e. about 10 Å). The energy scales c_{bl} for the bond length potential and c_{ba} for the bond angle potential are chosen as $c_{\mathrm{bl}} = 100$, $c_{\mathrm{ba}} = 10$. These choices of the parameters ensure that the chains are rather strongly stretched at the temperatures of interest (T of order ϵ and hence of order unity, choosing Boltzmann's constant $k_{\mathrm{B}} \equiv 1$). Note also that the rods cannot intersect each other during the simulations, using randomly and uniformly distributed displacements from a cubic box around the previous position (x, y, z) of an effective monomer ($x \pm \Delta$, $y \pm \Delta$, $z \pm \Delta$) as an attempted Monte Carlo move. The jump distance parameter Δ was chosen temperature and density dependent such that the average acceptance rate of these moves was about 50%.

In the present paper we applied the NAT ensemble throughout; that is, the area $A = L_xL_y$ of the substrate was held fixed, and the conjugate variable, the spreading pressure π_A, then can be calculated using the virial theorem.[51] The third linear dimension L_z was chosen distinctly larger than the length of the stretched chain, which ensures that there are no finite size effects caused by this choice. We choose the planar linear dimensions of the box according to $L_x/L_y = 2/\sqrt{3}$, which allows a perfect triangular lattice of the head groups in the plane $z = 0$. This is appropriate for the "nontilt" structure and the fluid phase, but causes problems in the case of the "uniform tilt" structure, where it is known[6−8,10,11] that the triangular head group lattice is distorted into a centered rectangular lattice. This distortion is also expected for the present model, as calculations in the $N\pi_AT$

ensemble show.[16] Suppressing this distortion by fixing $L_x/L_y = 2/\sqrt{3}$ (and choosing periodic boundary conditions to avoid the disturbances associated with free boundaries) has the effect that the components of the pressure tensor in x and y directions become nonequivalent, as will be seen below.

Despite these systematic problems, we use here the NAT ensemble, since equilibration is considerably faster than in the $N\pi_A T$ ensemble.[15,16] At each temperature 20 000 Monte Carlo steps (MCS) per effective monomer are carried out for equilibration, and at least 50 000 MCS for taking averages (only every 500 MCS are the system configurations analyzed, to avoid too strong correlations between these configurations, so that data are based on averages over 100 individual configurations for each combination of parameters). Near the critical temperature of the transition from the "uniform tilt" to the "no tilt" phase, substantially longer runs were needed because of "critical slowing down".[41−43] Although we use a link-cell algorithm,[51] the rather large interaction range ($d_{LJ} = 2$) and the complicated potential (eqs 1−4) require substantial computation for each attempted Monte Carlo move, and hence the CPU time requirements of the present work were substantial (on the order of 10^3 h on IBM 6000/370 RISC workstations). Even then the maximum size simulated was only 11 200 effective monomers (corresponding to 1600 fatty acids with about 20 CH_2 groups each). While this number of degrees of freedom still is several orders of magnitude less than what is feasible for lattice problems (for example, for phase separation of polymer blends on the order of 10^5 effective monomers were used[52]), it is about 1 order of magnitude larger than what is used for chemically detailed models.[23−34]

In any case even for this simplified model one has to be very careful in asserting the nature of the phase structure, since there is a subtle competition between intramolecular (bond length and bond angle) potentials and the Lennard-Jones forces, in addition to the possible misfit created by the size and shape of the simulation box. As an example of the problems that occur, Figures 2 and 3 compare snapshot pictures of a system of 100 chains with $l = 7$ at $T = 0.2$ at two neighboring coverages $\rho = 1.253$ ($L_x = 9.6$, Figure 2) and $\rho = 1.307$ ($L_x = 9.4$, Figure 3). Both systems have been started at $T = 0.1$ in a state of uniform tilt toward the next nearest neighbor of the triangular lattice of the head groups in the plane $z = 0$. While this state is maintained for the case of the lower density (cf. also the corresponding Voronoi diagram), in the case of the higher density the system has switched over to a state with uniform tilt toward the nearest neighbor direction (Figure 3). While at small enough densities all monomers of the same layer (labeled by the index i of the effective monomers along a chain) lie roughly in the same plane, this is no longer possible for high densities, where monomers can no longer all be in the minima of both the bond length potential and Lennard-Jones potential simultaneously. Due to this "frustration" a modulation of the height of the monomers above the surface occurs, which is quite evident from the snapshot pictures (compare the smooth surface of the layer in Figure 2 with the more corrugated one in Figure 3). But these effects are very sensitive to size and shape of the simulation box, and one sometimes also has to fight against pronounced hysteresis effects resulting from other boundary-induced defects. And while experimentally indeed both phases with uniform tilt toward nearest neighbors and toward next nearest neighbors have been observed,[6−8,10,11] due to the limitations of the present study, we refrain from making hasty statements about the full phase diagram of the present model. Somewhat simpler, of course, is the one-dimensional case where the "uniform tilt" to "no tilt" transition exists in the ground state as well, and a rounded version of this transition persists at finite temperatures (see the Appendix).

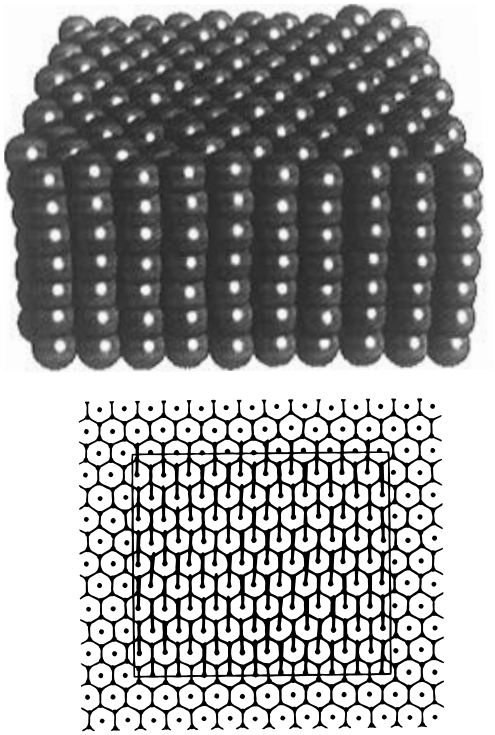

Figure 2. Snapshot picture (a, top) and corresponding Voronoi diagram (b, bottom) for a system of 100 chains with $l = 7$ effective monomers at a temperature $T = 0.2$ and at a coverage of $\rho = 1.253$. Each effective monomer is represented by a sphere of diameter unity. In the Voronoi diagram the projection of the "director" (i.e. the vector connecting the head group (denoted by a dot) and the end monomer of the surfactant molecule) is shown by a straight line in the xy-plane, together with the Voronoi tesselation for the head group lattice. Note that here the tilt is in the $+y$ direction (i.e., away from the spectator in part a and thus difficult to recognize visually).

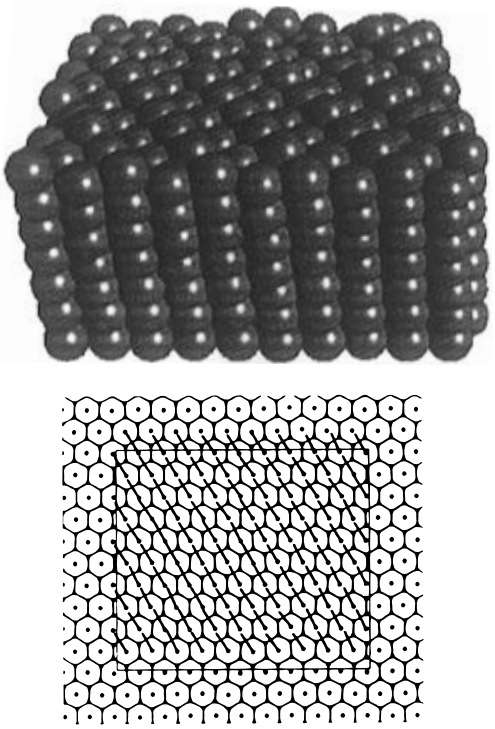

Figure 3. Same as Figure 2 but for the coverage $\rho = 1.307$. A tilt in the nearest neighbor direction of the triangular lattice is easily recognized from both the snapshot picture (a, top) and the projection of the director (b, bottom).

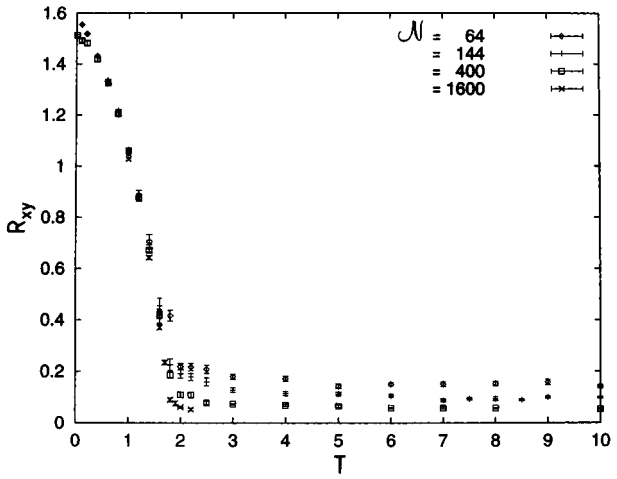

Figure 4. Order parameter R_{xy} plotted vs temperature for a coverage $\rho = 2/\sqrt{3} = 1.155$ and four choices of the number of surfactant molecules N as indicated. Data refer to $l = 7$ effective monomers.

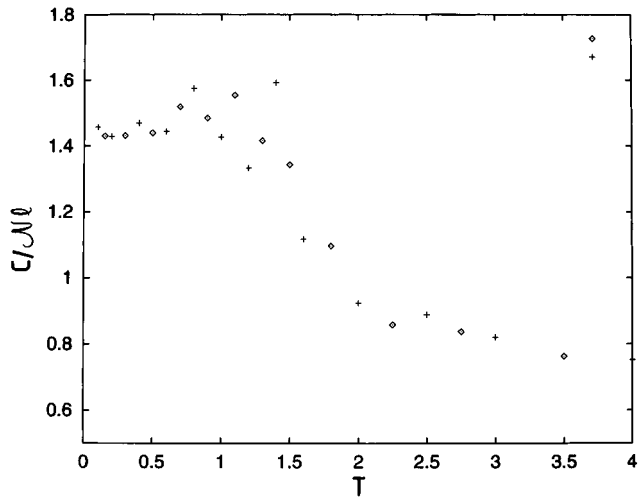

Figure 5. Specific heat C/Nl per effective monomer plotted vs temperature for the choice $l = 7$, $N = 144$, $\rho = 1.155$. Crosses show data extracted from the standard fluctuation relation from fluctuations of the internal energy E, while diamonds are data obtained from a numerical differentiation of the $\langle E \rangle$ vs T curve.

3. Finite Size Scaling Analysis of the Phase Transition from the "Uniform Tilt" to the "No Tilt" Structure

As is well-known, phase transitions can only occur in the thermodynamic limit, while in finite size systems transitions are rounded and shifted.[53,54] However, finite size scaling theory[53,54] has become a valuable tool for the extrapolation of data from very small systems to the thermodynamic limit, and this analysis of finite size effects has become a standard method for the study of various phase transitions.[41−43] Hence we apply these concepts also for the orientational phase transition of surfactant monolayers here.

We need to introduce an order parameter that distinguishes between the "uniform tilt" and the "no tilt" phases. For this purpose, we first consider an average of the end-to-end vector $\vec{e}_\nu$ of the individual chains, $\vec{e}_\nu = (l_{\nu x}, l_{\nu y}, l_{\nu z})$,

$$\vec{e} = (1/N) \sum_{\nu=1}^{N} \vec{e}_\nu \tag{5}$$

where N is the total number of surfactants in our model system. The root mean square projection of this average end-to-end vector into the xy-plane is then defined by taking a configurational average $\langle ... \rangle$ as follows:

$$R_{xy} = \langle (e_x^2 + e_y^2) \rangle^{1/2} \tag{6}$$

Note that in the ordered phase there are six equivalent tilt directions (considering an ordering where uniform tilt in the direction of next nearest neighbors of the triangular head group lattice occurs, as is the case for the ground state of our model[13]). The quantity R_{xy} is independent of this tilt direction. Note that in a finite system quantities such as $\langle e_x \rangle$, $\langle e_y \rangle$ vanish identically[41−43,53,54] since there is always a nonzero probability that the system jumps from one of the six degenerate orientations to another one (even if for a short run such a state with a specific orientation might be metastable, this problem is of practical relevance always near the second-order transition). Thus quantities such as $\langle e_x \rangle$, $\langle e_y \rangle$ are unsuitable to study this transition, while R_{xy} is of order unity in the regime of the ordered phase and of order $1/\sqrt{N}$ in the disordered phase. This is a trivial consequence of the self-terms $e_{\nu x}^2 + e_{\nu y}^2$ that appear when one works out R_{xy} from eq 6.

The numerical data (Figure 4) bear out these expectations very well. We have chosen here a coverage where the lattice spacing (a) of the triangular head group lattice also is $a = 1$. One can see that at low temperatures the order parameter R_{xy} is nearly independent of size, while at high temperatures there are pronounced finite size tails, which decrease with increasing N. Note that R_{xy} is not normalized to unity in the ground state [rather at $T = 0$ we have $R_{xy} = (l - 1)d_0 \sin \Theta_0$, for a chain with l effective beads (Figure 1) that have the length d_0 at $T = 0$, and Θ_0 is the angle between the director and the z -axis in the ground state[13]].

Of course, Figure 4 allows only a rough estimation of the transition temperature, since the curves for the different values of N start to broaden somewhat already in the region of the ordered phase. The situation is not better when one considers the specific heat C, which should show a peak near the transition. But Figure 5 shows only a very mild peak, and since with the chosen computational effort there are still large statistical errors, we have not attempted to analyze the specific heat as a function of N. The lack of a clear-cut peak in Figure 5 is evidence that the transition is second order and not first order (otherwise one would see a smeared out remnant of the delta function singularity representing the latent heat of the transition). The fact that two different methods to estimate C yield equivalent results is another check that thermal equilibrium has been reached,[41−43] which is a nontrivial finding for a complicated model like the present one, for which equilibration times may be huge and are difficult to assess a priori.

A more reliable estimation of the phase transition point T_c comes from the cumulant intersection method.[42,54] Defining the order parameter square $M^2 = e_x^2 + e_y^2$, we expect from the finite size scaling theory near T_c that moments $\langle M^{2k} \rangle$ depend on the temperature distance $1 - T/T_c$ and the linear dimension L basically via the scaled combination L/ξ, where the correlation length $\xi \propto |1 - T/T_c|^{-\nu}$,[53,54]

$$\langle M^{2k} \rangle = L^{-2k\beta/\nu} \tilde{M}_{2k}(L/\xi) \tag{7}$$

where $\tilde{M}_{2k}(L/\xi)$ is a scaling function which for large arguments behave as $\tilde{M}_{2k}(L/\xi) \propto (L/\xi)^{2k\beta/\nu}$ in order to yield $\langle M^{2k} \rangle_{L\to\infty} \propto \xi^{-2k\beta/\nu} \propto |1 - T/T_c|^{2k\beta}$, β being the order parameter exponent. Note however the suggestion[55] that the scaling function may contain nonuniversal elements when k is too large. Obviously the power law prefactor in eq 7 is constructed such that it ensures a sensible thermodynamic limit. The power law prefactors cancel, however, if we form suitable combinations of such

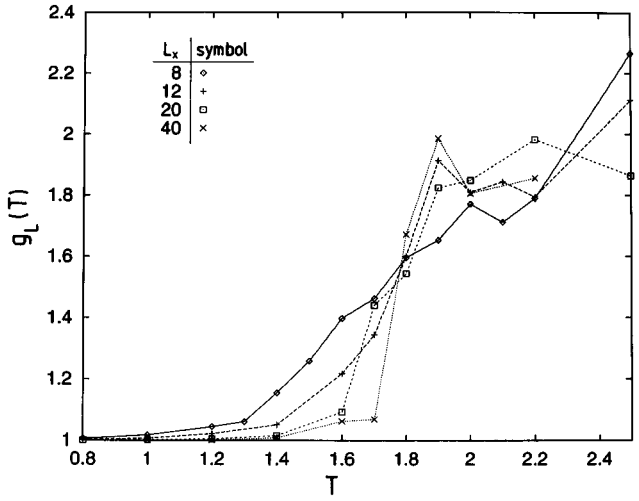

Figure 6. Unnormalized cumulant $g_L(T)$ plotted vs temperature for four different linear dimensions $L = L_x$ (remember $L_y = L_x\sqrt{3}/2$).

moments, such as the (unnormalized) fourth-order cumulant $g_L(T)$,[42,54]

$$g_L(T) \equiv \langle M^4\rangle/\langle M^2\rangle^2 = \langle (e_x^2 + e_y^2)^2\rangle/\langle e_x^2 + e_y^2\rangle^2 \qquad (8)$$

From eq 7 we recognize that near T_c $g_L(T)$ should be a function solely dependent on the ratio L/ξ, $g_L(T) = \tilde{g}(L/\xi)$. Since ξ diverges at T_c, curves $g_L(T)$ for different choices of L should intersect at T_c in a common intersection point. This "cumulant intersection method"[42,54] is well-known and established for the study of phase transitions in simple systems, but has not yet been applied to orientational transitions in surfactant monolayers. Figure 6 shows—despite considerable statistical scatter of the data—that the method is useful for the present problem, too, and we estimate the transition temperature as $T_c = 1.80 \pm 0.05$.

Comparing the behavior of the order parameter in Figure 4 to corresponding data for simple two-dimensional models such as Ising and Potts models,[41−43,53,54] we recognize characteristic differences: first of all, finite size effects are much less pronounced in Figure 4, and also the decrease of the order parameter with temperature is much less steep. All these observations indicate that in the present case the behavior is much closer to mean field theory (where $\beta = 1/2$) rather than in these standard models. The fact that $g_L(T_c) \approx 1.6$ is closer to the value 1.59 for the $d = 3$ Ising class[56] instead of the values 2.0 to 2.1 for the mean field universality class[57,58] does not change our conclusion because the convergence of g_L (T_c) often is rather slow.[59] Probably the reason for this mean field character is that in the present case each effective monomer interacts with many neighbors.

It is interesting to note that the order of the transition from uniform to no tilt phases does depend sensitively on the detailed degrees of freedom, which are included in the model, and the nature of the interactions: using rigid rods (rather than flexible chains as done here) grafted to a perfect lattice, Scheringer et al.[38] did obtain a first-order transition, while here we find a second-order transition. Note that both models include strong attractive forces between effective monomers and thus do not contradict the result[60] that there is no such transition with purely repulsive forces.[60]

4. Coverage Dependence of the "Uniform to No Tilt" Transition

The physical reason for the existence of tilted structures, of course, is that at low coverage by tilting of the chains the density

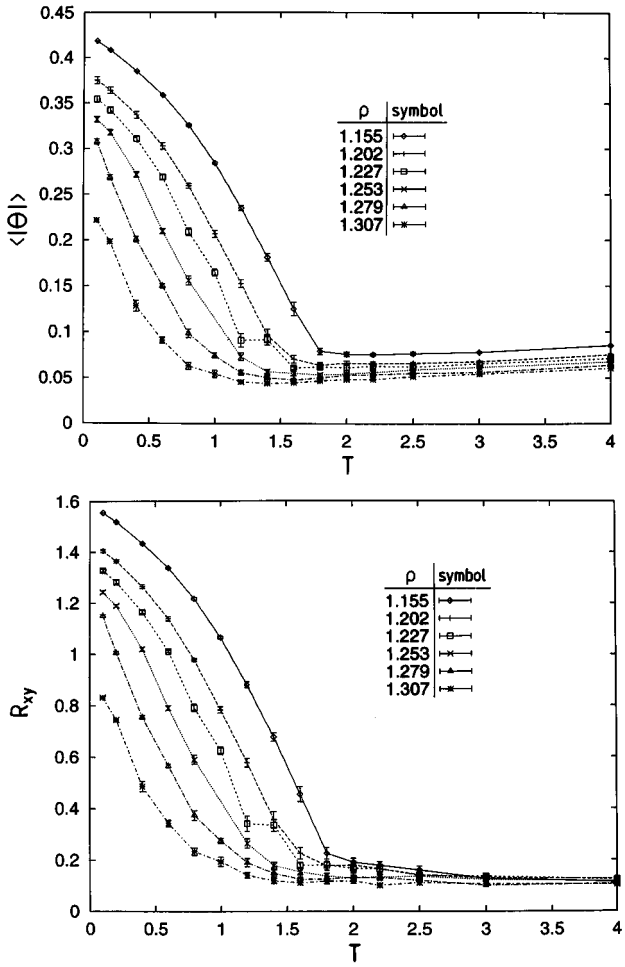

Figure 7. (a, top) Average of the absolute value of the tilt $\langle|\Theta|\rangle$ plotted vs temperature for various coverages as indicated for $l = 7$ and $N = 100$ molecules. Note that the nonzero value of $\langle|\Theta|\rangle$ in the no tilt phase simply results from the fact that in a finite system the probability distribution $P(\Theta)$ of the tilt angle is a Gaussian-centered zero but with a small nonzero width, and $\langle|\Theta|\rangle$ is of the same order as this width. (b, bottom) Order parameter R_{xy} plotted vs temperature T for various coverages as indicated.

in the monolayer increases as its height decreases, and in this way a lower energy state can be found. Conversely, when the coverage increases, also the density of the no tilt structure can get large enough such that the effective monomers sit in the minima of the Lennard-Jones potential of their neighbors.

This expectation is indeed borne out by our numerical simulations (Figure 7). One sees that both the tilt angle at $T = 0$ (where it is maximal) and the corresponding order parameter $R_{xy}(T=0)$ decrease with increasing coverage, so the tendency of the system to develop a tilted structure is less pronounced the higher the density. Consequently also the critical temperature T_c for the transition from the uniform tilt structure to the no tilt structure decreases with increasing coverage. From the ground state analysis presented previously[13] we know that at $T = 0$ the transition occurs at a coverage of $\rho_c \approx 1.804$. This is a much larger coverage than analyzed in Figure 7.

It is also interesting to note that the transition to the no tilt phase gets more and more rounded as the coverage increases. This fact indicates that fluctuations are then more pronounced. In our opinion this instability of the system against fluctuations is related to the fact that a corrugated structure with uniform tilt in nearest neighbor direction (Figure 3) may be more stable than the usual structure with tilt in next nearest neighbor direction (Figure 2). Only the latter has been included in the ground state analysis of ref 13, and since there is also an obvious

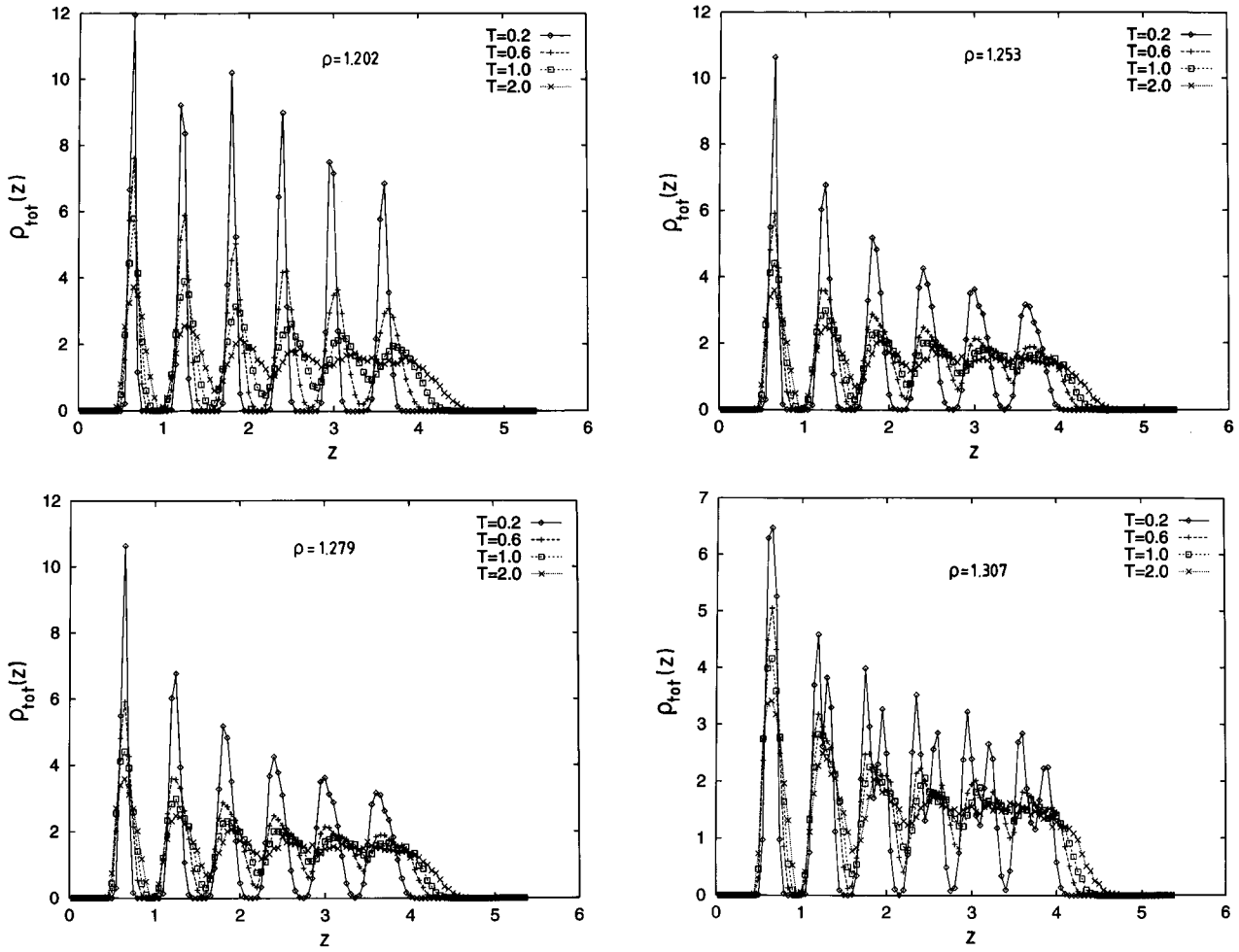

Figure 8. Total monomer density profiles $\rho_{tot}(z)$ in the z direction for $l = 7$ at four temperatures as indicated in the figure, for coverages $\rho = 1.202$ (a, top left), 1.253 (b, top right), 1.279 (c, bottom left) and 1.307 (d, bottom right). Note the splitting of the peaks corresponding to the individual layers at the highest coverage at $T = 0.2$. Note that all density profiles are normalized such that $\int_0^\infty dz \rho_{tot}(z) = l - 1$ excluding the effective monomer at $z = 0$.

problem of distinguishing which of these phases is truly thermodynamically stable and which of them is only metastable, we cannot yet present a reliable phase diagram. But we note that the corrugated structure is also easily recognized from a different behavior of the monomer density profiles (Figure 8). In the uniform tilt structure, there are pronounced peaks for the individual layers $i = 1, 2, ..., l - 1$ corresponding to the labels of the effective monomers along each chain, and these peaks are well separated from each other by distinct minima. In the no tilt phase, however, these minima are washed out in the exterior region of the monolayer (only near the grafting plane $z = 0$ is the layered structure stabilized by the boundary condition that the first effective monomer representing the head group is fixed precisely at the surface plane). For the corrugated structure of Figure 3, however, we recognize that each individual layer is split into a double peak structure (Figure 8d).

It is also interesting to analyze the spreading pressure in our model system. Note that the spreading pressure is a (2×2) tensor,

$$\underline{\pi}_A = \begin{pmatrix} \pi_A^{xx} & \pi_A^{xy} \\ \pi_A^{yx} & \pi_A^{yy} \end{pmatrix} \tag{9}$$

where the off-diagonal component $\pi_A^{xy} = \pi_A^{yx}$ represents the shear forces. From the virial theorem (the symbol $\otimes$ stands for a tensorial product)

$$\underline{\pi}_A A = N k_B T \underline{1} + \langle \sum_i \vec{r}_i \otimes \vec{F}_i \rangle NAT \tag{10}$$

one can readily obtain $\underline{\pi}_A$ calculating the forces F_i on particle i from the respective potentials. One can show that intramolecular potentials do not contribute to the spreading pressure.[22,61] While in the fluid phase there are no shear components and $\underline{\pi}_A$ is simply proportional to the unit tensor $\underline{1}$, this is not necessarily true in the solid phases in the *NAT* ensemble, because by fixing the linear dimensions L_x, L_y a priori we may strain the "natural" structure of the system, and hence $\pi_A^{xx} \neq \pi_A^{yy}$ may result. Figure 9 shows that the pressure is isotropic in the no tilt phase but becomes anisotropic in the uniform tilt structure, the component π_A^{yy} being then consistently higher (note that y is the direction of the tilt, and x the direction normal to the tilt). In fact, negative values of π_A^{xx} for low temperatures and low coverages in Figure 9a indicate that the structure with $L_x/L_y = 2/\sqrt{3}$ then is not thermodynamically stable but only metastable. Fixing such a ratio of linear dimensions, one could expect phase separation into a low-coverage (two-dimensional) gas and the high-coverage equilibrium structure in the thermodynamic limit: of course, due to unfavorable boundary effects (and too small observation times), such phase separation was never observed in our studies. We have observed however long-lived defect structures induced through the boundaries. In any case, these findings are an indication that, in principle, simulations in the $N\pi_A T$ ensemble should be preferred; they should more easily yield thermal equilibrium. Such simulations have

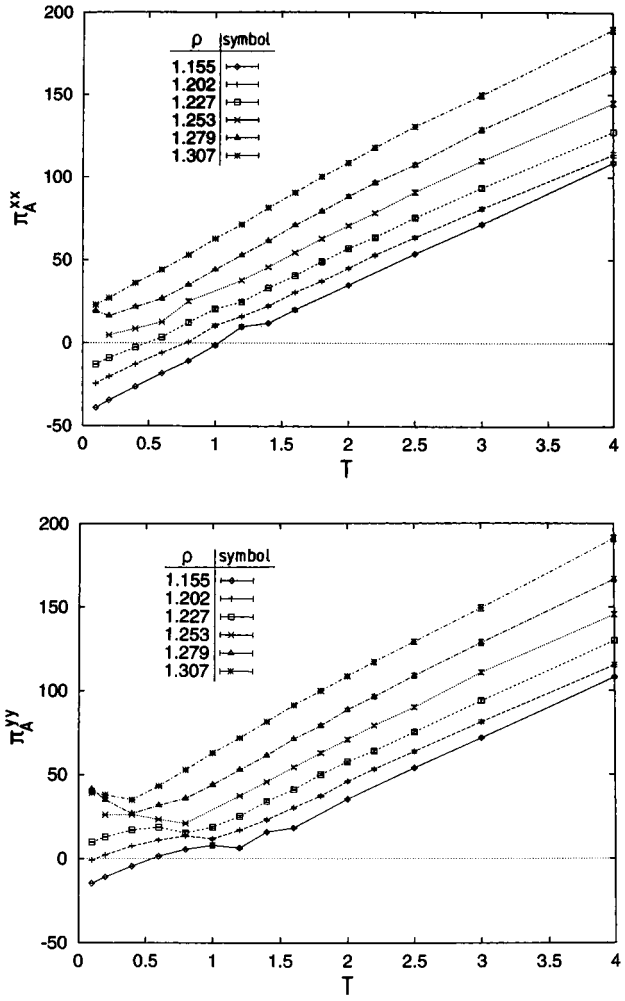

Figure 9. Spreading pressure components π_A^{xx} (a, top) and π_A^{yy} (b, bottom) plotted vs temperature for $l = 7$ and various coverages.

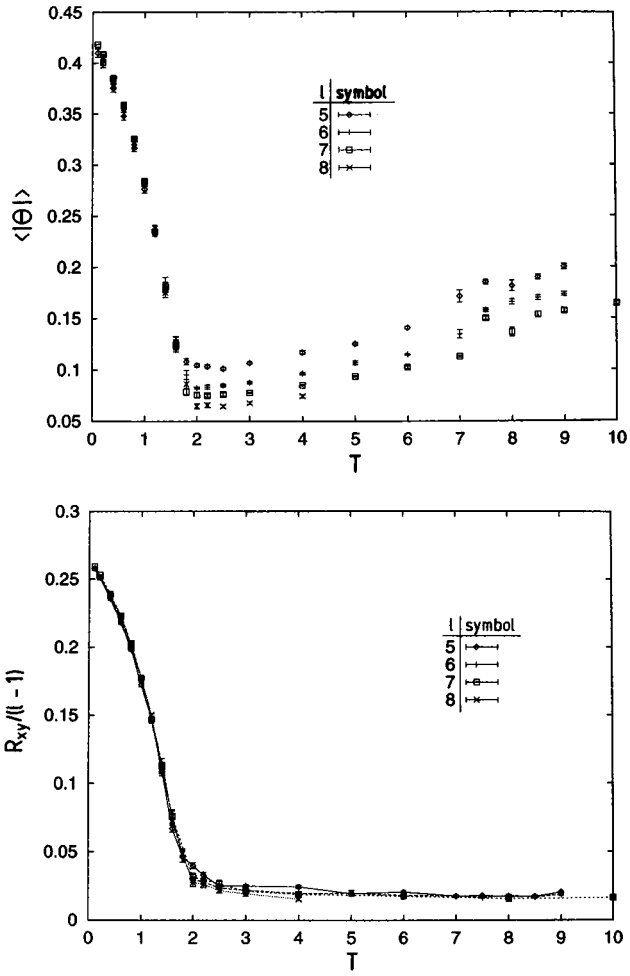

Figure 10. Average of the absolute value of the tilt angle $\langle|\Theta|\rangle$ (a, top) and order parameter per bond $R_{xy}/(l - 1)$ (b, bottom) plotted vs temperature, at a coverage $\rho = 1.155$ and four choices of l as indicated.

been carried out for the present problem,[16] but unfortunately, they are considerably more demanding in computer time. The onset of a difference $\pi_A^{xx} - \pi_A^{yy}$ in Figure 9 can again be taken as a rough indication of the transition temperature.

5. Chain Length Dependence of the "Uniform to No Tilt" Transition

A variation of the chain length of the alkane chains is interesting, since it is established from experiment that for fatty acids there is a linear increase of phase transition temperatures with chain length.[8,10] While such an effect has readily been reproduced with the rigid rod model of ref 38, it turns out that in the present model the transition temperature to a good approximation is independent of chain length (Figure 10). At fixed coverage, both the average tilt angle $\langle|\Theta|\rangle$ and the order parameter per bond $R_{xy}/(l - 1)$ practically superimpose independent of l. Analysis of the spreading pressure shows (Figure 11) that π_A^{xx}, π_A^{yy} increase with increasing l in the no tilt phase, while near the transition temperature there is rather little dependence of the spreading pressure on chain length, and in the uniform tilt phase the tendency is opposite, longer chains exhibiting lower pressure.

We can only speculate why the present model does not show any tendency for an increase of the transition temperature with chain length. One possible reason is that the stabilization of the structure by fixing the head groups in the plane $z = 0$ is more effective the shorter the chains. This effect is obvious when one compares the density profiles (Figure 12), where a fluid-like layer (constant density) occurs on top of the monolayer for the temperature $T = 2.0$ for $l = 7$ and $l = 8$, while for $l = 5$ and $l = 6$ the layering effect caused by the first head group plane at $z = 0$ has not yet fully decayed. Such an effect is not expected to be present for real fatty acids at the air−water interface, of course, where the natural roughness of such an interface should allow significant fluctuations of the head groups in the vertical direction as well. Suppressing these fluctuations artificially, as done in our model, very likely raises transition temperatures of the ordered phases, and this effect is expected to be more pronounced the thinner the surfactant monolayer is. Another possible source of less stability of thin layers is a possible conflict between the interactions among head groups as compared to interactions among the monomers of the alkane chains. Thus the discrepancies between our model and experiment give rather plausible directions for future improvement of the model.

6. Concluding Remarks

In the present work, we have given a first orientation about the phase behavior of a coarse-grained model for surfactant monolayers at surfaces, such as fatty acids at the air−water interface. Attention was focused on the transition from the "uniform tilt" to the "no tilt" structure of the layer (an additional transition from a solid to a liquid state occurs in this model as well,[13,16] but for the chosen parameters this transition occurs at a distinctly higher temperature, and it is not discussed further in the present paper). We have studied, in the *NAT* ensemble,

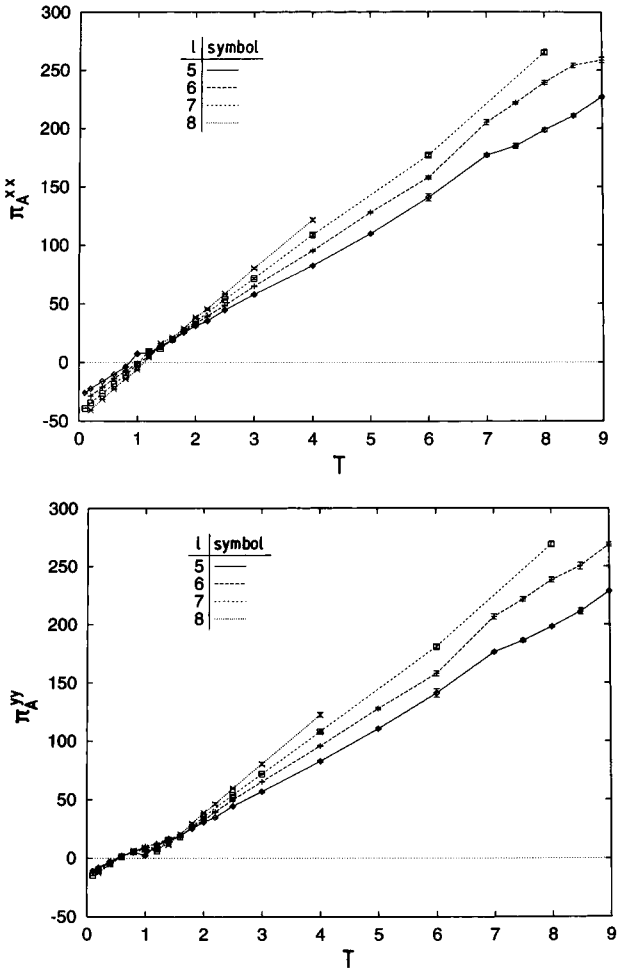

Figure 11. Spreading pressure components π_A^{xx} (a, top) and π^{yy} (b, bottom) plotted vs temperature for $N = 100$, $\rho = 1.155$, and four different chain lengths as indicated.

how this orientational phase transition depends on both the density and the chain length of the molecules.

The present model has the advantage that it is simple enough so one can analyze[13] rather straight-forwardly the ground state phase diagram at $T = 0$, use the knowledge of the ground state structure as an initial condition for Monte Carlo runs at low temperatures, and thus generate well equilibrated system configurations. We have shown that it is feasible to apply then the standard techniques to analyze phase transitions from simulations of small systems, such as the cumulant intersection technique motivated by the finite size scaling approach.

A serious problem of the *NAT* ensemble is the fact that in the "uniform tilt" phase the spreading pressure gets anisotropic, since in an unconstrained system the perfect triagonal head group−lattice is not the equilibrium structure, but rather this lattice structure gets distorted into a centered rectangular lattice. The periodic boundary condition of the *NAT* ensemble enforces a perfect triangular lattice at low temperatures, however. While we can locate the phase boundary from the "no tilt" structure to the "uniform tilt" structure, possible further transitions at lower temperature (changes in tilt orientation, for instance) cannot be reliably investigated. In principle, this problem is avoided by the use of the $N\pi_A T$ ensemble, but at the expense of a much higher computational effort.[16] Nevertheless this ensemble is also preferable for a study of the melting transition at higher temperatures: the strong increase of π_A at constant A shows that in reality the model would show a strong expansion of the layer with increasing temperatures if π_A is held fixed (at a physically realistic value).

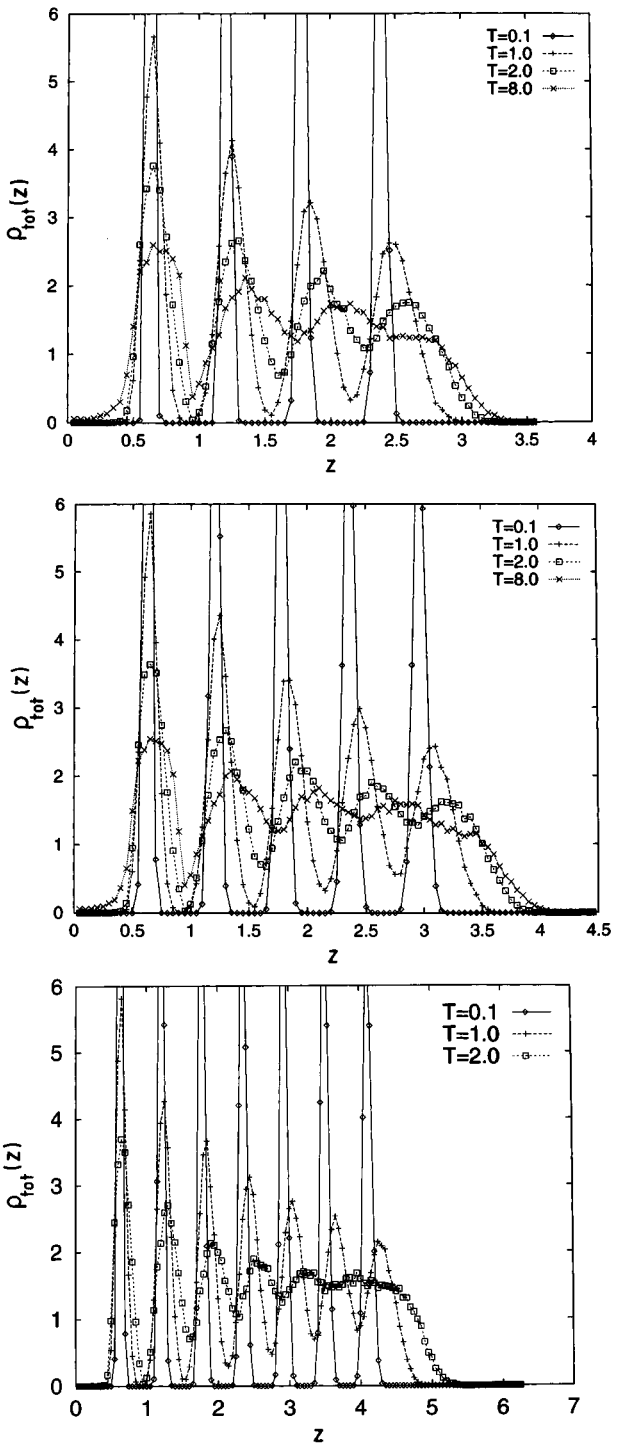

Figure 12. Total monomer density profiles $\rho_{tot}(z)$ in the z direction for a coverage $\rho = 1.155$ and several temperatures as indicated in the figure, for $l = 5$ (a, top), $l = 6$ (b, middle), and $l = 8$ (c, bottom). All profiles are normalized such that $\int_0^\infty dz \rho_{tot}(z) = l - 1$, excluding the effective monomer at $z = 0$.

Thus it is clear that the present work can be viewed as a first step only, and improvement of the model is desirable in several directions. We have already emphasized that it is clearly too crude to make the head groups virtually identical to the effective monomers: in future work, we hence plan to study the competition that arises when the Lennard-Jones parameters of the head groups prefer a different lattice spacing than the Lennard-Jones parameters of the effective monomers. Proceeding with such step-by-step improvements, it will be possible to identify the detailed mechanisms underlying the structure and physical properties of real surfactant monolayers.

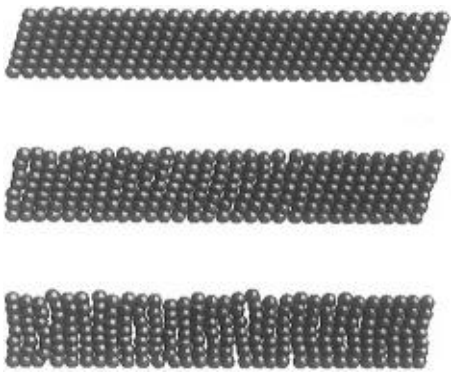

Figure 13. Snapshot pictures of the one-dimensional model with $L_x = 30$, $l = 7$, and three temperatures: $T = 0.1$ (a, top), $T = 0.8$ (b, middle) and $T = 2$ (c, bottom).

Acknowledgment. We are grateful to H. Möhwald, C. Helm, and I. R. Peterson for useful discussions. One of us (F.M.H.) received partial support from the Graduiertenkolleg "Physik und Chemie supramolekularer Systeme" der Deutschen Forschungsgemeinschaft (DFG). This work was also supported by the Materialwissenschaftliches Forschungszentrum Mainz (MWFZ).

Appendix: The One-Dimensional Model

For the sake of completeness and in order to provide a comparison, also the one-dimensional variant of the model has been studied. The snapshot pictures (Figure 13) and the variation of the order parameter (Figure 14) again give evidence for a "uniform tilt" structure at low temperatures which gradually disorders as the temperature is raised. Of course, on general grounds one expects that at $T > 0$ in one dimension uniform

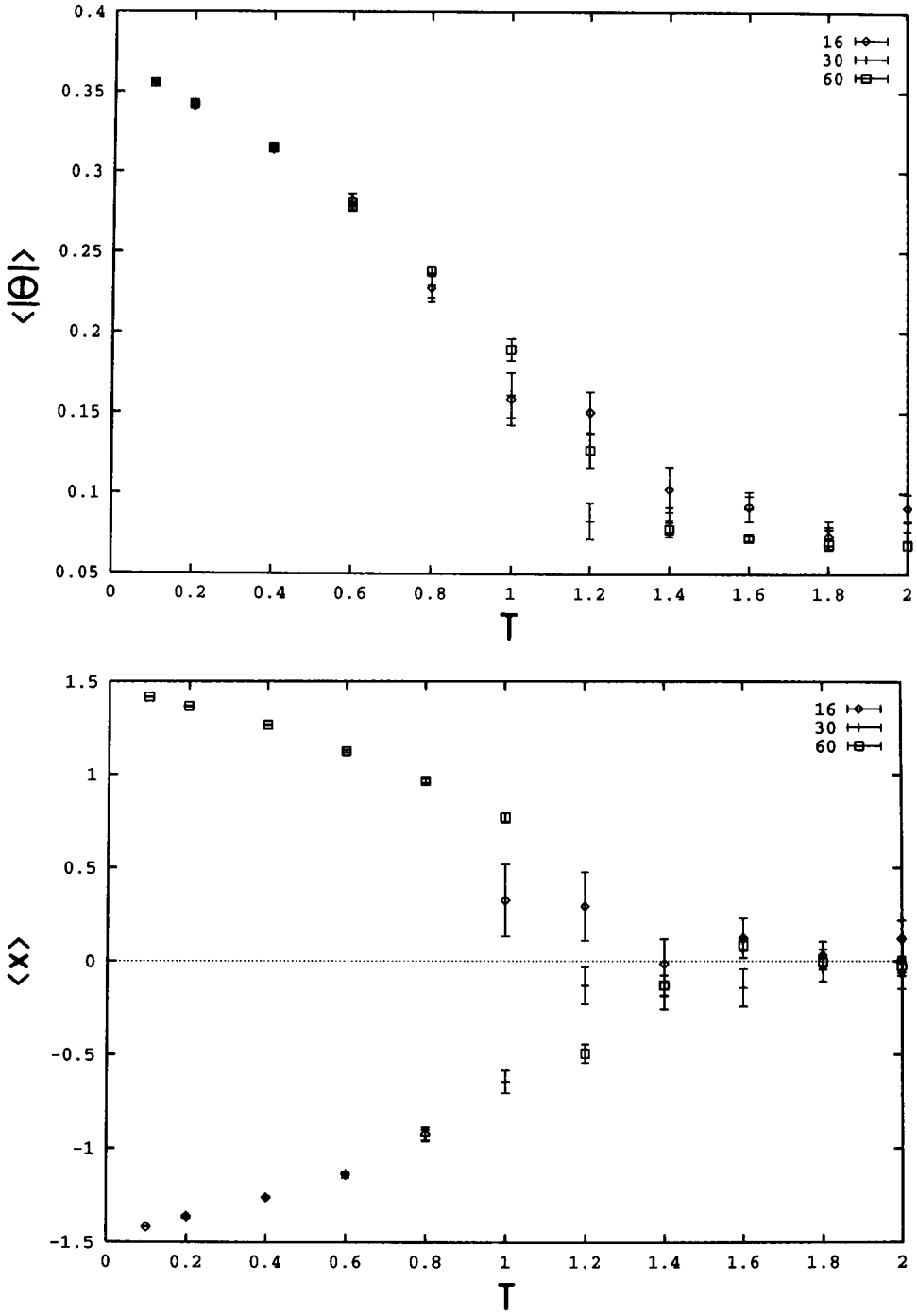

Figure 14. Average tilt angle (a, top) and order parameter $\langle x \rangle$ (average x-component of the end-to-end vector of the chain) (b, bottom) plotted vs temperature, for three choices of the system linear dimension L_x as indicated.

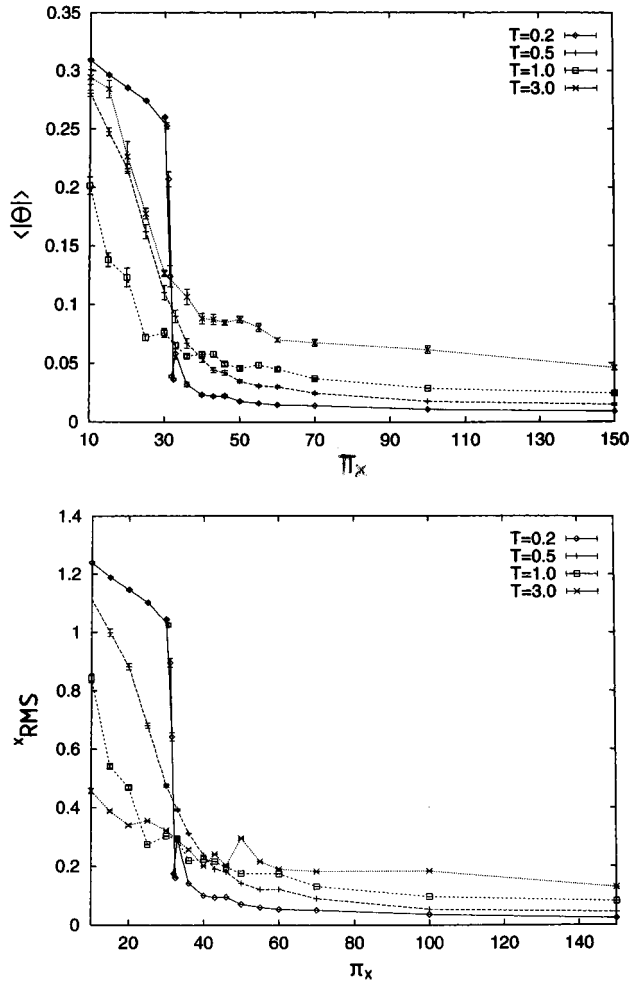

Figure 15. Average tilt angle (a, top) and root mean square order parameter X_{RMS} (b, bottom), XRMS $= \langle (N^{-1}\sum_{i=1}^{N} x_i)^2 \rangle^{1/2}$, plotted vs spreading pressure π_x in the one-dimensional case, for $N = 30$ and four temperatures as indicated.

tilt order at $\pm\Theta$ is unstable against the spontaneous formation of kinks,[36] so domains with positive tilt angle $+\Theta$ and negative tilt angle $-\Theta$ should alternate. However, at low temperatures the average domain size $\langle l_d \rangle$ is clearly much larger than the linear dimension L_x chosen here, and thus the probability to have a kink−antikink pair in the system is very small at the temperatures of interest.

It is also interesting to study the ordering at fixed temperatures as a function of the spreading pressure π_x (which is a scalar quantity here); see Figures 15 and 16. The behavior at the lowest temperature shown ($T = 0.2$) resembles a first-order transition at $\pi_x \approx 32$, while at higher temperature the decrease of the order parameter X_{RMS} with increasing spreading pressure is rather smooth. As mentioned above, in principle this variation should be smooth at all nonzero temperatures, while the behavior at $T = 0.2$ presumably is a remnant of the zero-temperature behavior. As expected, this "transition" at $T = 0.2$ is rather sensitive to the size of the system,[15] but large statistical fluctuations prevented us from performing a more detailed analysis. Isotherms (Figure 16) are rather smooth, they exhibit less structure than recent theories of one-dimensional lipid models suggest,[62] and hence they do not allow a straightforward conclusion on the ordering behavior of the system, however.

Finally, Figure 17 shows the variation of the tilt angle with the distance between the head groups (which is nothing but $\langle L_x \rangle / N$, of course). It is seen that for low density (large $\langle L_x \rangle / N$) the behavior at finite temperature is rather similar to the ground state results, while near the transition from the "no tilt" to the "uniform tilt" structure the variation at nonzero low temperature is much more steep.

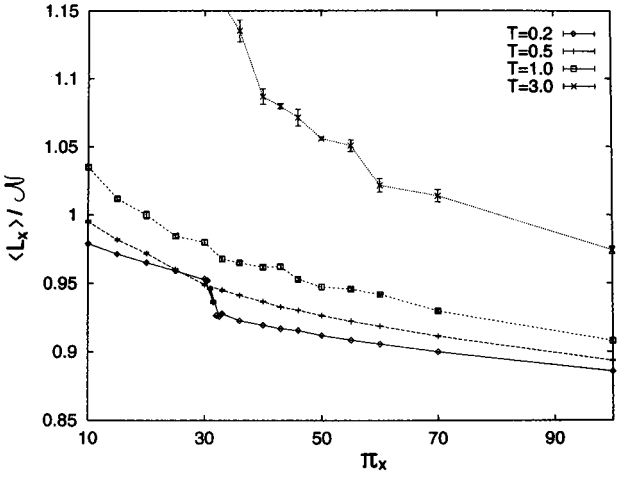

Figure 16. Average linear dimension per molecule, $\langle L_x \rangle / N$, plotted vs spreading pressure for $N = 30$, $l = 7$, and four different temperatures.

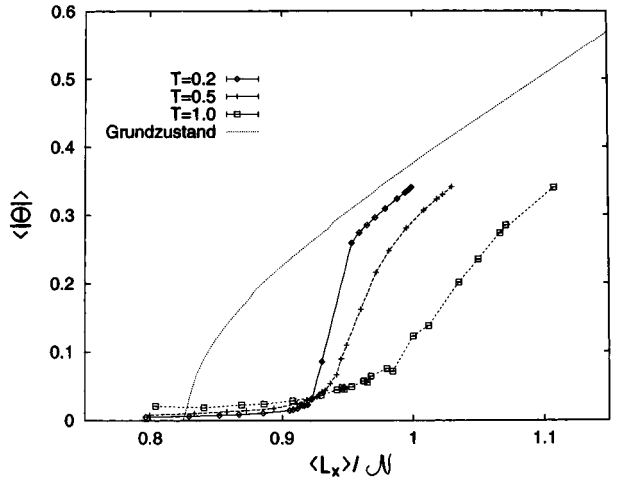

Figure 17. Average of the absolute value of the tilt plotted vs average linear dimension per molecule, $\langle L_x \rangle / N$, for four temperatures as indicated. All data are for $N = 30$ and $l = 7$.

References and Notes

(1) Gaines, G. L., Jr. *Insoluble Monolayers at Liquid-Gas Interfaces*; Interscience: New York, 1996.
(2) Knobler, C. M. In *Advances in Chemical Physics*; Rice, S. A., Ed.; Wiley: New York, 1988; p 397.
(3) Grunze, M.; Kreuzer, H., Eds. *Adhesion and Friction*; Springer: Heidelberg, 1989.
(4) Möhwald, H. *Annu. Rev. Phys.* **1990**, *41*, 441.
(5) Ulman, A. *An Introduction to Ultrathin Organic Films*; Academic: San Diego, 1991.
(6) Knobler, C. M.; Desai, R. C. *Annu. Rev. Phys. Chem.* **1992**, *43*, 207.
(7) Andelman, D.; Brochard, F.; Knobler, C. M.; Rondelez, F. In *Micelles, Membranes, Microemulsions, and Monolayers*; Gelbart, M., Ben Shaul, A., Roux, D., Eds.; Springer: Berlin, 1994; p 559.
(8) Bibo, A.; Peterson, I. *Adv. Mater.* **1990**, *2*, 309.
(9) Lin, B.; Shih, M. C.; Bonahon, T. M.; Ice, G. E.; Dutta, P. *Phys. Rev. Lett.* **1990**, *65*, 191.
(10) Bibo, A.; Knobler, C. M.; Peterson, I. *J. Phys. Chem.* **1991**, *95*, 2092.
(11) Kenn, R., et al. *J. Phys. Chem.* **1991**, *95*, 5591.
(12) Kaganer, V. M.; Loginov, E. B. *Phys. Rev. Lett.* **1993**, *71*, 2599.
(13) Haas, F. M.; Hilfer, R.; Binder, K. *J. Chem. Phys.* **1995**, *102*, 2960.
(14) Hilfer, R.; Haas, F. M.; Binder, K. *Nuovo Cimento* **1994**, *D16*, 1297.
(15) Haas, F. M. Dissertation, Johannes Gutenberg Universität Mainz, unpublished.
(16) Haas, F. M.; Hilfer, R. *J. Chem. Phys.*, in press.

(17) Binder, K. *Macromol. Chem., Macromol. Symp.* **1991**, *50*, 1.
(18) Baschnagel, J.; Binder, K.; Paul, W.; Laso, M.; Suter, U.; Batoulis, J.; Jilge, W.; Bürger, T. *J. Chem. Phys*. **1991**, *95*, 6014.
(19) Baschnagel, J.; Qin, K.; Paul, W.; Binder, K. *Macromolecules* **1992**, *25*, 3117.
(20) Binder, K. In *Monte Carlo and Molecular Dynamics Simulations in Polymer Science*; Binder, K., Ed.; Oxford University Press: New York, 1995; p 3.
(21) Tries, V.; Paul, W.; Baschnagel, J.; Binder, K. Preprint.
(22) Leontidis, E.; Forrest, B. M.; Widmann, A. H.; Suter, U. W. *J. Chem. Soc., Faraday Trans.* **1995**, *91*, 2355.
(23) Harris, J.; Rice, S. A. *J. Chem. Phys.* **1988**, *89*, 5898.
(24) Egberts, E.; Berendsen, H. *J. Chem. Phys*. **1988**, *89*, 3718.
(25) Bareman, J. B.; Cardini, G.; Klein, M. L. *Phys. Rev. Lett*. **1988**, *60*, 2125. Cardini, G.; Bareman, J. B.; Klein, M. L. *Chem. Phys. Lett*. **1988**, *145*, 493.
(26) Hautman, J.; Klein, M. L. *J. Chem. Phys*. **1989**, *91*, 4994; *Ibid.* **1990**, *93*, 7483.
(27) Bareman, J. B.; Klein, M. L. *J. Phys. Chem*. **1990**, *94*, 5202. Hautman, J.; Bareman, J. B.; Mar, W.; Klein, M. L. *J. Chem. Soc., Faraday Trans*. **1991**, *87*, 2031.
(28) Bishop, M.; Clarke, J. H. R. *J. Chem. Phys*. **1991**, *95*, 540.
(29) Moller, M. A.; Tildesley, D. J.; Kim, K. S.; Quirke, N. *J. Chem. Phys*. **1991**, *94*, 8390.
(30) Karaborni, S.; Toxvaerd, S. *J. Chem. Phys.* **1992**, *96*, 4965; *Ibid.* **1992**, *96*, 5505.
(31) Karaborni, S.; Toxvaerd, S.; Olsen, O. *J. Phys. Chem*. **1992**, *96*, 4965.
(32) Collazo, N.; Shin, A.; Rice, S. A. *J. Chem. Phys.* **1992**, *96*, 4735. Shin, S.; Collazo, N.; Rice, S. A. *J. Chem. Phys.* **1992**, *96*, 1352.
(33) Alper, H.; Basolino, D.; Stouch, T. *J. Chem. Phys.* **1993**, *98*, 9798.
(34) For an introductory review, see: Tobias, D. J.; Tu, K.; Klein, M. L. In *Monte Carlo and Molecular Dynamics Simulations of Condensed Matter Systems*; Binder, K., Ciccotti, G., Eds.; Societa Italiana di Fisica: Bologna, 1996; p 325.
(35) Safran, S. A.; Robbins, M. O.; Geroff, S. *Phys. Rev.* **1986**, *A33*, 2186.
(36) Kreer, M.; Kremer, K.; Binder, K. *J. Chem. Phys*. **1990**, *92*, 6195.
(37) Milik, M.; Kolinski, A.; Skolnick, J. *J. Chem. Phys.* **1990**, *93*, 6.
(38) Scheringer, M.; Hilfer, R.; Binder, K. *J. Chem. Phys.* **1992**, *96*, 2269.
(39) Stettin, H.; Mögel, J. H.; Friedemann, R. *Ber. Bunsen-Ges. Phys. Chem.* **1993**, *7*, 44.
(40) Haas, F. M.; Lai, P.-Y.; Binder, K. *Makromol. Chem., Theory Simul*. **1993**, *2*, 889.
(41) Binder, K., Ed. *The Monte Carlo Method in Condensed Matter Physics*; Springer: Berlin, 1992.
(42) Binder, K.; Heermann, D. W. *Monte Carlo Simulation in Statistical Physics: An Introduction*, 2nd ed.; Springer: Berlin, 1992.
(43) Binder, K., Ciccotti, G., Eds. *Monte Carlo and Molecular Dynamics Simulations of Condensed Matter Systems*; Societá Italiana di Fisica: Bologna, 1996.
(44) Chakrabarti, A.; Toral, R. *Macromolecules* **1990**, *23*, 2016.
(45) Lai, P. Y.; Binder, K. *J. Chem. Phys*. **1991**, *95*, 9288; *Ibid*. **1992**, *97*, 586.
(46) Grest, G. S.; Murat, M. in ref 20, Chapter 9.
(47) Hoehner, G.; Kinzler, M.; Wöll, Ch.; Grunze, M.; Scheller, M. K.; Cederbaum, L. S. *Phys. Rev. Lett*. **1991**, *67*, 851.
(48) Outka, D. A.; Stöhr, J.; Rabe, J. P.; Swalen, J. D. *J. Chem. Phys.* **1988**, *88*, 4076.
(49) Kinzler, M.; Schertel, A.; Höhner, G.; Wöll, Ch.; Grunze, M.; Albrecht, H.; Holzhüter, G.; Gerber, Th. *J. Chem. Phys.* **1994**, *100*, 7722.
(50) Gau, C. S.; Yu, H.; Zagrafi, G. *Macromolecules* **1993**, *26*, 2524.
(51) Allen, M. P.; Tildesley, D. J. *Computer Simulation of Liquids*; Clarendon Press: Oxford, 1987.
(52) Deutsch, H.-P.; Binder, K. *Macromolecules* **1992**, *25*, 6214.
(53) Privman, V., Ed. *Finite Size Scaling and the Numerical Simulation of Statistical Systems*; World Scientific: Singapore, 1991.
(54) Binder, K. *Finite Size Effects on Phase Transitions* In *Computational Methods in Field Theory*; Gausterer, H., Lang, C. B., Eds.; Springer: Berlin, 1992; p 59.
(55) Hilfer, R. *Z. Phys.* **1994**, *B96*, 63.
(56) Ferrenberg, A. M.; Landau, D. P. *Phys. Rev.* **1991**, *B44*, 5081.
(57) Binder, K.; Nauenberg, M.; Privman, V.; Young, A. P. *Phys. Rev.* **1985**, *B31*, 1498.
(58) Brézin, E.; Zinn-Justin, J. *Nucl. Phys*. **1985**, *B257*, 867.
(59) Mon, K. K.; Binder, K. *Phys. Rev.* **1993**, *E48*, 2498. Luijten, E.; Blöte, H. W. J. Preprint.
(60) Somoza, A. M.; Desai, R. J. *J. Phys. Chem*. **1992**, *96*, 1401.
(61) Ciccotti, G.; Ryckaert, J. P. *Comput. Phys. Rep*. **1986**, *4*, 345. Gao, J.; Weiner, J. *J. Chem. Phys*. **1989**, *90*, 6749; *Ibid*. **1989**, *91*, 3168.
(62) Gianotti, R. D.; Grimson, M. J.; Silbert, M. *J. Phys. A: Math. Gen*. **1992**, *25*, 2889.

JP9610980